Progress In Electromagnetics Research M, Vol. 89, 141–149, 2020

T-Shaped I/O Feed Based Differential Bandpass Filter with Symmetrical Transmission Zeros and High Common Mode Rejection Ratio

Rida Gadhafi[1, *], Dan Cracan[2], Ademola A. Mustapha[2], and Mihai Sanduleanu[3]

Abstract—A T-shaped feed based differential microstrip bandpass filter (BPF) with high common-mode (CM) rejection ratio is presented. The filter comprises two magnetically coupled conventional square open-loop resonators (SOLRs), with capacitive coupled T-shaped input-output (I/O). The choice of the T-shaped I/O coupling feed enables a higher common-mode suppression of −57 dB at f_0^d that extends up to $4.1f_0^d$ with a value better than −30 dB. Frequency f_0^d is the cutoff frequency of the differential-mode (DM) passband. Moreover, this feed can symmetrically position two transmission zeros (TZs) at the upper and lower stopbands. This yields a highly selective and compact filter. Additionally, a T-shaped feed only excites the odd mode of the filter resulting in a wide stopband with high out of band rejection. The upper and stopband rejection of the filter is better than −50 dB. To demonstrate the design, DM and CM lumped models of the filter are proposed and studied. The filter operates at 1.263 GHz with a fractional bandwidth (FBW) of 3.9%. The design is validated experimentally by characterizing DM, CM, common-mode to differential-mode (CD), and differential-mode to common mode (DC). Moreover, the group delay (GD) response of the filter is measured, and a significantly flat response is observed with a maximum delay variation of only 0.88 ns in the 3 dB bandwidth.

1. INTRODUCTION

Microstrip bandpass filters with distributed element components are widely used in modern wireless communication systems. The design approach for building microstrip filters with coupled resonators makes the filter design procedure simple and routine [1]. Numerous examples of such filters can be seen in the literature [1–10]. The filter selectivity of such filters is improved by imposing one or more transmission zeros that are obtained by utilizing the cross-coupling between adjacent resonators [1–3]. However, this method can increase the size of the filter rendering a more expensive filter with a larger real estate on the PCB. Moreover, sharp transition band filters are susceptible to common-mode to differential mode perturbations. That is why high CM rejection is required for those filters [7]. In addition, a balanced bandpass filter should also exhibit strong out-of-band rejection and high selectivity. Inspired by [7], the differential filter design was initialized with a pair of magnetically coupled open loop resonators. Magnetic coupling was chosen because of its inherent property to suppress the CM transmission. As the resonators are magnetically coupled, the excitation will be capacitive in nature. However, the traditional capacitive excitation, with a constant gap, gives poor out of band rejection and a very narrow band CM suppression [8]. For improving the performance, such designs require additional modifications of the resonators, with the expense of increasing the order of the filter. Contrary to this,

Received 18 November 2019, Accepted 14 January 2020, Scheduled 2 February 2020

* Corresponding author: Rida Gadhafi (rgadhafi@ud.ac.ae).

[1] College of Engineering and IT (CEIT), Department of Engineering, University of Dubai, United Arab Emirates. [2] Department of Electrical and Computer Engineering, Khalifa University, United Arab Emirates. [3] System on Chip Center (SoCC), Department of Electrical and Computer Engineering, Khalifa University, United Arab Emirates.

the paper proposes a simple technique to enhance the CM rejection over a wide band range, without modifying the open loop resonator. A T-shaped, I/O coupling feed is used here together with the magnetically coupled open loop resonators. This, then, enables a higher CM suppression of −57 dB at f_0^d that extends up to $4.1f_0^d$ with a value better than −30 dB, where f_0^d is the cutoff frequency of the DM passband. Moreover, the cross-coupling of the resonators to this feed can symmetrically position two transmission zeros at the upper and lower stopbands producing a narrower transition band, with extra out of band rejection. As a result of cross-coupling, the group delay curve becomes flat. A maximum group delay variation of only 0.88 ns is observed in the measured group delay within the 3 dB bandwidth. Additionally, this type of feed only excites odd modes and suppresses even modes occuring in the loop resonator filter design. To demonstrate the design, DM and CM lumped models of the filter are proposed and studied. The BPF filter operates at 1.263 GHz with FBW of 3.9%. The differential mode (DM), common-mode (CM), common-to-differential (CD), differential-to-common (DC), and Group-Delay (GD) characteristics are evaluated. This paper is organized as follows. Section 2 describes the structure and the design of a T-shaped I/O coupled bandpass filter. A parametric study is included as well. Section 3 explains the S-parameter characterization of the proposed filter along with the group delay measurement. A benchmark table and a comparison discussion is introduced in Section 4 followed by conclusions in Section 5.

2. OPEN-LOOP COUPLED RESONATOR WITH T-SHAPED I/O FEED

2.1. Filter Structure

The proposed microstrip differential bandpass filter, T-shaped feed, and equivalent circuit are shown in Fig. 1(a). The filter comprises conventional magnetically coupled resonators. The structure follows a plane of symmetry at XX1. As the coupling is magnetic, the feed for an intrinsic filter will be capacitive in nature [7]. T-shaped capacitive excitations are used shown in Fig. 1(b) [11]. As shown, the feed is symmetrical at MM1, and l_T represents the perimeter of the feed. The proposed filter is microstrip in nature and fabricated on an FR-4 substrate ($\epsilon_r = 4.4$, $\tan\delta = 0.02$, substrate thickness = 1.6 mm). The

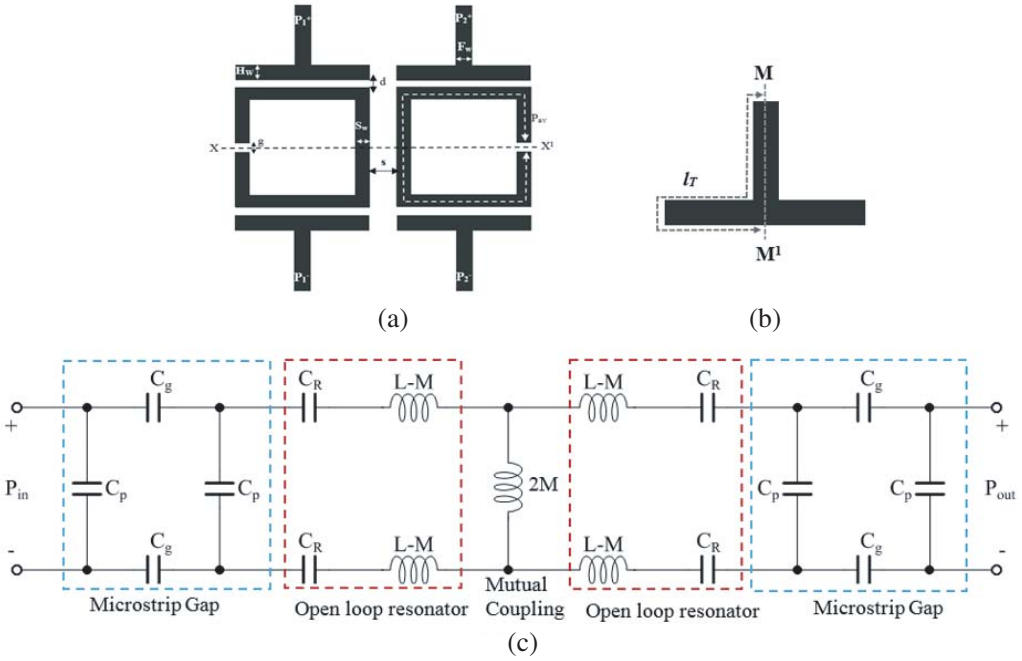

Figure 1. Structure of the proposed differential bandpass filter with T-shaped I/O feed. (a) Differential filter structure, XX1 represents the plane of symmetry, (b) T-Shaped Feed along with its equivalent circuit, (MM1 represents the plane of symmetry), (c) equivalent circuit of the differential filter shown in Fig. 1(a).

filter design is performed by using a full-wave 3D electromagnetic (EM) simulator (ANSYS HFSS). The fabricated filter is characterized on an Agilent Network Analyzer (PNA-X, N5242A).

2.2. Design

Figure 2 shows the comparison of magnetically coupled resonator filter with tapped feed and the proposed T-shaped feed. Both single ended and differential responses of the proposed filter are demonstrated. In contrast to a normal tapped feed, the T-shaped feed can introduce a transmission zero at the lower stopband frequency. As depicted, single ended loop resonator filters will have higher order modes — both even and odd modes of the fundamental frequency. However, T-shaped feed can excite only odd modes of the fundamental frequency producing a wide stopband region as shown in Fig. 2. The T-shaped feed excites the resonator symmetrically, and only odd modes are excited, thus suppressing even modes that occur in the conventional loop resonator filter design. As stated, the classical magnetically coupled filter has the second harmonic of the fundamental mode. For a tapped feed, even though a transmission zero appears in the upper stopband, the lower stopband experiences poor out of band rejection. In the case of T-shaped feed filter, cross-coupling to this type of feed can introduce two transmission zeros (TZs), T_{z1} and T_{z2}, at the lower and upper stopband frequencies F_{tz1} and F_{tz2}, respectively. This is a method for controlling the filter bandwidth and the roll off of the transition band. Simulations show that T_{z1} is due to the capacitive nature of the feed, and T_{z2} is created due the proposed T-shaped feed.

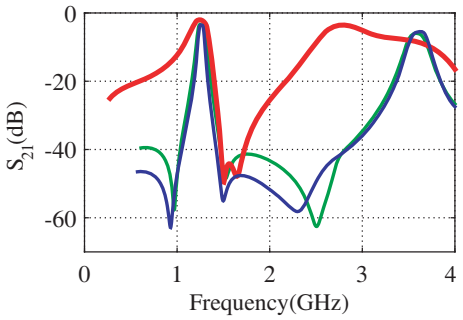

Figure 2. Comparison of classical magnetically coupled singled ended filter to that of T-shaped filter with single ended and differential configuration. Green, Red, and Blue lines represent single ended filter with T-shaped feed, single ended filter with tapped feed and differential filter with T-shaped feed respectively.

The frequency position of the two TZs can be varied from parameter l_T.

Figure 3 shows the filter response along with the transmission zeros for different values of l_T. The frequencies of the two transmission zeros are:

$$F_{tz2} = \frac{c}{4l_T\sqrt{\epsilon_{eff}}} \tag{1}$$

$$F_{tz1} = \frac{1}{2\pi\sqrt{L_T C_G}} \tag{2}$$

In Eq. (1), c is the speed of light and ϵ_{eff} the effective permittivity, and in Eq. (2), L_T is the inductance of the input T feed and C_G the capacitance of the gap ($C_G = \epsilon L_{feed} t_{cop}/d$). It can be noticed that the position of the first transmission zero can be modified in tandem with the second one through the geometry of the input feed or independently through the gap between the input feed and the resonator. These equations are validated by parametric simulations. Thus, as shown in Fig. 3, TZs can be controlled by the perimeter in Fig. 3 without affecting the center frequency of the filter. As already shown in Fig. 1(a), the leg of the 'T' is a 50 ohm microstrip transmission line, and the top of the 'T' is electromagnetically coupled with one of the resonating edges of the open loop resonator.

Three different types of feeding structures have been simulated: L-shaped, inverted L-shaped, and T-shaped ones. Corresponding DM and CM responses are shown in Fig. 4. As seen in Fig. 4(a), the

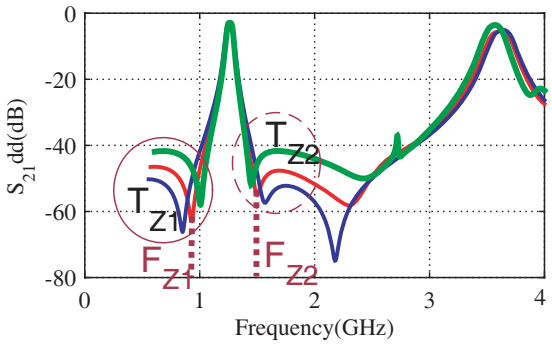

Figure 3. Positioning of transmission zeros with T-shaped feed for different dimensions of l_T. (a) filter response.

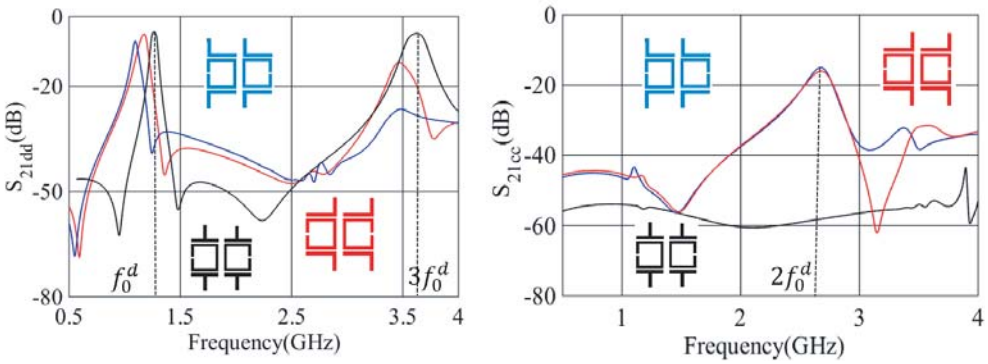

Figure 4. Simulated DM and CM responses of the proposed filter for different shapes of I/O feed; T-shaped, L-shaped and inverted L-shaped feed. (a) DM and b) CM.

two TZs at the lower and upper stopbands make the transition band narrower, with high out of band rejection. The lower and upper stopband rejections of the filter are better than −50 dB. As depicted in Fig. 4(b), T-shaped feed enables high common mode rejection at passband that extends up to $4.1f_0^d$. The feed allows a symmetrical excitation of the loop resonators causing rejection of the common mode and significantly improving the differential mode. As seen, the amount of CM suppression of the L-shaped and inverted L-shaped feeds is not as high as the T-shaped feed and has a peak at $2f_0^d$.

In addition to the T-shaped feed, another key element in the proposed design is the magnetically coupled SOLRs (two of them are used here). As shown in Fig. 1(c), this equivalent circuit is modeled by including the effect of the microstrip coupling gap, d. In Fig. 1(c), C and L represent self-capacitance and self-inductance, whereas M represents the mutual inductance. The fundamental resonant frequency of SOLR can be written as:

$$f_c = \frac{c}{2(P_{av} - g)\sqrt{\epsilon_{eff}}} \tag{3}$$

In Eq. (3), P_{av} is the average perimeter of the square loop, and g is the gap between the open ends. A tight coupling between two resonators causes mode splitting and increased bandwidth [12]. Hence, the gap s is chosen to have weakly coupled resonators with narrowband characteristics. However, a strong I/O coupling can reduce the insertion loss in the passband. Hence, the coupling gap d between the resonating arm and feed is chosen to be 0.3 mm after considering the fabrication tolerance. The proposed feeding structure can be used to implement single-ended and differential bandpass filters. The coupling coefficient k of both single-ended and differential filters can be extracted using the method discussed in [13].

$$k = \frac{f_{m1}^2 - f_{m2}^2}{f_{m1}^2 + f_{m2}^2} \tag{4}$$

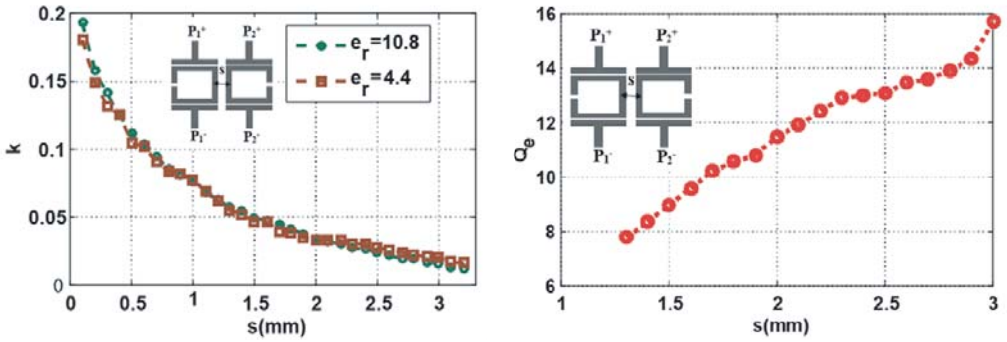

(a) (b)

Figure 5. Coupling coefficient (k) and external quality factor of the differential open loop resonator filter with T shape feed, (a) k on different dielectric constant substrates, (b) Q_e as a function of coupling distance, s.

In Eq. (4), f_{m1} and f_{m2} are the two resonant peaks of the magnetically coupled loop resonators. The extracted coupling coefficient of a differential filter for two different dielectric materials is shown in Fig. 5(a). As shown, magnetic coupling has an independence of dielectric constant, enabling easy design techniques for different dielectric substrates. The extracted external quality factor as a function of coupling distance s is shown in Fig. 5(b). A quality factor of 16 is required for producing FBW of 3.9%. The resonating frequency of the filter is at 1.263 GHz with a fractional bandwidth (FBW) of 3.9%. The insertion loss (IL) is 4 dB for the lossy FR-4 material used. This can be mitigated by using low loss materials, e.g., Rogers. The structure has been redesigned on Rogers, and it is found that the insertion loss is reduced to 2 dB. It is found from simulation that gap g between the open ends can be adjusted for a proper tuning of the filter. An average frequency shift of 32 MHz is expected for a change in the gap g of 1 mm. Thus, the proposed design permits a maximum tuning of 450 MHz bandwidth through gap adjustment.

3. EXPERIMENTAL CHARACTERIZATION

To characterize the differential filter, it is beneficial to calculate the mixed-mode S-parameters. By definition, mixed-mode S-parameters matrix is [14]:

$$S_M = \begin{vmatrix} S_{dd11} & S_{dd12} & S_{dc11} & S_{dc12} \\ S_{dd21} & S_{dd22} & S_{dc21} & S_{dc22} \\ S_{cd11} & S_{cd12} & S_{cc11} & S_{cc12} \\ S_{cd21} & S_{cd22} & S_{cc21} & S_{cc22} \end{vmatrix} \tag{5}$$

Based on this mixed-mode matrix, the proposed filter has been characterized in the following four different sets, and the results are analyzed. DC quadrant represents the electromagnetic susceptibility of the device as it degrades the signal-to noise ratio of the device. The measurement is conducted with the help of a four-ports Vector Network Analyzer (VNA) as shown in Fig. 6.

3.1. Differential-Mode Response(DD)

Figure 7 shows the simulated and measured differential-mode responses of the proposed filter. The size of the intrinsic filter is $0.192\lambda_g \times 0.315\lambda_g$ (25 mm × 41 mm, where λ_g is the guided wavelength of the bandpass filter at the operating frequency). The design parameters used for this design are: $H_w = F_w = S_w = 3$ mm, $g = 0.4$ mm, $s = 3.1$ mm, and $l = 19$ mm, where the optimum width of the T-shaped feed as well as the width of the loop resonator is kept the same to have maximum electromagnetic coupling of the structure. The measured DM center frequency is 1.263 GHz. The 3 dB bandwidth of the proposed filter is 3.9%, and the minimum insertion loss is 4 dB. The measured curve rolled-off faster than the simulated one due to higher unloaded external quality factor.

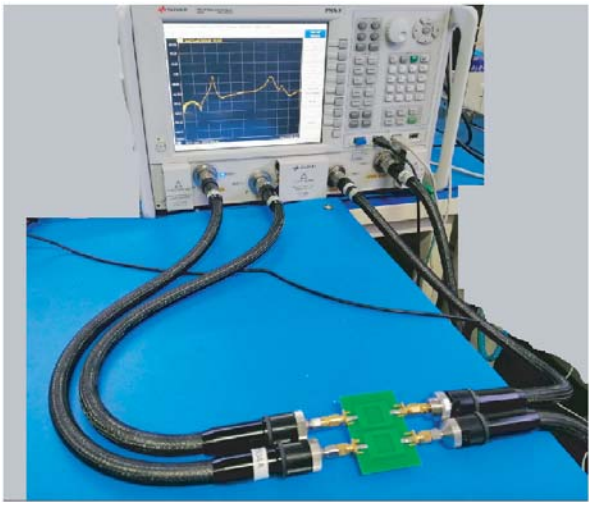

Figure 6. Measurement set-up of the proposed filter for differential S-parameter characterization.

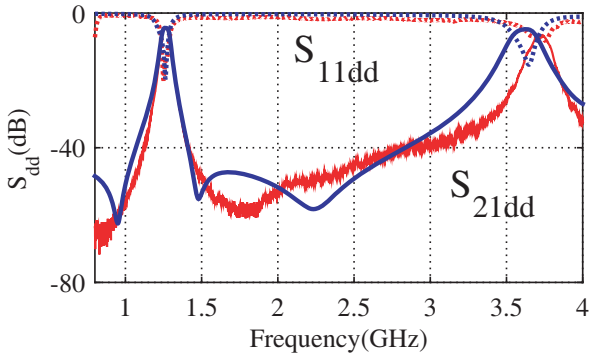

Figure 7. Simulated and measured DM responses of the proposed filter. Solid line represents measurement and dotted line represents simulation.

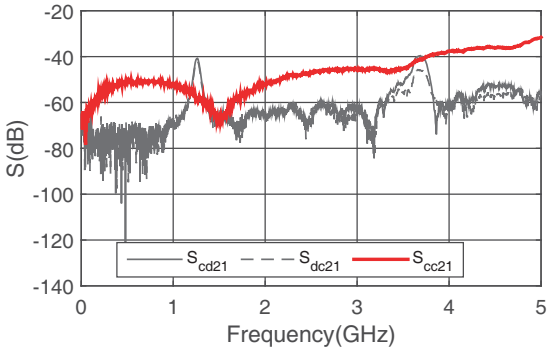

Figure 8. Measured transmission coefficient of CC, CD and DC.

3.2. Common-Mode Response

Figure 8 shows the measured CC response of the proposed differential bandpass filter. As seen, the measured and simulated CM rejection is between -55 and -57 dB within the 3 dB bandwidth of the differential passband. From simulation and measurement, a CM suppression better than -40 dB is achieved up to $4f_0^d$, where f_0^d is the center frequency of the differential passband. As previously stated, this can be attributed to the use of a T-shaped symmetrical I/O coupled line.

3.3. Common-Mode to Differential-Mode Response (CD)

Figure 8 shows CD transmission coefficient ((S_{cd21}) measurement result. As seen, it is very low (better than -60 dB from $0 - 0.92f_0^d$, $= -42$ dB at f_0^d and better than -60 dB from $1.07f_0^d$–$2.63f_0^d$). The Common-Mode Rejection Ratio (CMRR) can be defined as follows [15]:

3.4. Differential-Mode Response(DD)

$$\mathrm{CMRR}_{dB} = 20\log\frac{|S_{dd21}|}{|S_{cd21}|} \tag{6}$$

Equation (6) is used to calculate the CMRR of the proposed differential bandpass filter. The filter has a maximum CMRR of −57 dB at f_0^d.

3.5. Differential-Mode to Common-Mode Response(DC)

The differential to CM transmission coefficient (S_{dc21}) is shown in Fig. 8. As seen, it has the same performance as (S_{cd21}). The simulated and measured Group-Delays (GDs) of the proposed filter are shown in Fig. 9. It is clear that measured GD is higher than simulated GD due to the presence of external components like cables, connectors, etc. As seen in Fig. 9(b), near the transition areas of the filter, slight group delay variation can be seen. However, it is very small (0.88 ns for measured and 1 ns for simulated) allowing a flat response over the frequency band of interest. This highlights another advantage of the proposed differential filter for data transmission systems: it will eliminate the need for group delay equalizers in the system.

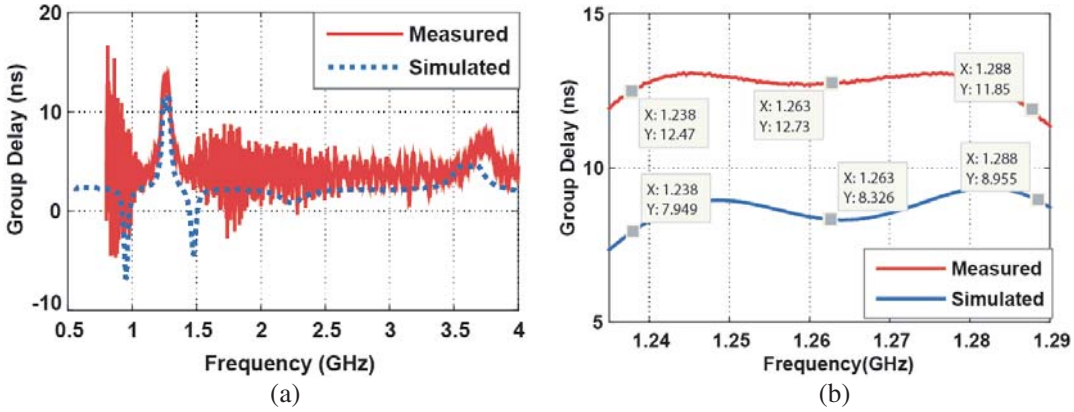

Figure 9. Group delay curve of the proposed filter. (a) Simulated and measured group delay responses. (b) Zoomed response with in the 3 dB bandwidth. Markers indicate 3 dB points and f_0^d.

4. BENCHMARK AND DISCUSSION

The differential filter discussed in this article is summarized and compared with the published data in Table 1. Note that the proposed filter offers higher CMRR in the passband (−57 dB) and a wider stopband that extends up to $4.1f_0^d$. Moreover, CD and DC (seldom tested in most of the articles in

Table 1. Benchmark between the proposed design and reported works.

Ref.	Technology	f_0^d (GHz)	CMRR at f_0^d (dB)	FBW (%)	$\lvert S_{cc21}\rvert \geq$ 30 dB	$\lvert S_{dc21}\rvert$ & $\lvert S_{dc21}\rvert \geq$ 30 dB	Max. GD variation in passband (ns)
This work	FR-4	1.263	57	3.9	0–$4.1f_0^d$	0–$4.1f_0^d$	0.88
[2]	$\epsilon_r = 2.65$	1	40	22.9	0–$2.9f_0^d$	N/A	N/A
[6]	$\epsilon_r = 3.5$	1.029	40	9.83	0–$3.7f_0^d$	N/A	N/A
[7]	FR-4	2.475	47	13.9	0–$2.29f_0^d$	N/A	N/A
[8]	Duroid	1.03	50	6.5	-	N/A	N/A
[9]	$\epsilon_r = 5.6$	2.45 & 5.6	47.2 & 30.2	7 & 9	0–$1.55f_0^d$	N/A	N/A

literature) capabilities of the proposed filter are also tested. We find that the proposed filter has a larger stopband rejection (below −40 dB). One of the significant parameters in all filter designs for modulated data transmission is the amount and shape of GD produced by the filter in the passband. As depicted in Table 1, contrary to all other previous studies, GD is tested for the proposed filter, and it is found that the filter produces almost a flat response within the 3 dB bandwidth with a maximum possible variation of 0.88 ns. In addition, the proposed filter has narrowband with FBW of 3.9%. As already stated, this performance is obtained with a compact design of the filter.

5. CONCLUSION

A differential microstrip bandpass filter with high common mode suppression is presented. The filter comprises two magnetically coupled square open-loop resonators with capacitive coupled T-shaped input-output (I/O). The novelty lies in the choice of a T-shaped input-output coupling feed, which enables a higher CM suppression of −57 dB at f_0^d that extends up to $4.1f_0^d$ with a value better than −30 dB, where f_0^d is the cutoff frequency of the DM passband. Moreover, we find that this feed can symmetrically position two TZs at the upper and lower stopbands rendering a compact and highly selective filter. Additionally, T-shaped feed only excites the odd mode of the filter resulting in a wide stopband with high out of band rejection. The upper and stopband rejection of the filter is greater than 50 dB. The proposed filter operates at 1.263 GHz with an FBW of 3.9%. Contrary to previous studies, the proposed design is fully validated experimentally by characterizing all possible transfers (DM, CM, CD, and DC). Moreover, the group delay of the filter is measured, and a significantly flat response is observed with a maximum group delay variation of only 0.88 ns in the 3 dB bandwidth. The proposed filter can find its application in RF front ends where differential input and output with high CM suppression are required.

REFERENCES

1. Hong, J-S. and M. J. Lancaster, "Couplings of microstrip square open-loop resonators for cross-coupled planar microwave filters," *IEEE Trans. Microwave Theory Tech.*, Vol. 44, 1019–1021, 1996.
2. Feng, W., W. Che, and Q. Xue, "Balanced filters with wideband common mode suppression using dual-mode ring resonators," *IEEE Transactions on Circuits And Systems — I: Regular Papers*, Vol. 62, No. 6, 1499–1507, 2015.
3. Prieto, A. F., et al., "Compact balanced dual-band bandpass filter with magnetically coupled embedded resonators," *IET Microwaves, Antennas & Propagation*, Vol. 13, No. 4, 492–497, 2019.
4. Garcia, R. G., R. L. Sanchez, D. Psychogiou, and D. Peroulis, "Multi-stub-loaded differential-mode planar multiband bandpass filters," *IEEE Trans. on Circuits and Systems — I: Express Briefs*, Vol. 65, No. 3, 271–275, 2018.
5. Gao, X., W. Feng, and W. Che, "High selectivity wideband balanced filters using coupled lines with open/short stubs," *IEEE Microwave Wireless Compon. Lett.*, Vol. 27, No. 3, 260–262, 2017.
6. Cervantes, J. L. O. and A. C. Chavez, "Microstrip balanced bandpass filter with compact size, extended-stopband and common-mode noise suppression," *IEEE Microwave Wireless Compon. Lett.*, Vol. 23, 530–532, 2013.
7. Prieto, A. F., A. Lujambio, J. Martel, F. Medina, F. Mesa, and R. R. Boix, "Simple and compact balanced bandpass filters based on magnetically coupled resonators," *IEEE Trans. Microwave Theory Tech.*, Vol. 63, 1843–1853, 2015.
8. Deng, H. W., L. Sun, F. Liu, Y. F. Xue, and T. Xu, "Compact tunable balanced bandpass filter with constant bandwidth based on magnetically coupled resonators," *IEEE Microwave and Wireless Components Letters*, Vol. 29, No. 4, 2019.
9. Xiao, J. K., X. B. Su, H. X. Wang, and J. G. Ma, "Compact microstrip balanced bandpass filter with adjustable transmission zeros," *Electronics Letters*, Vol. 55, No. 4, 212–214, 2019.

10. Wu, C. H., C. H. Wang, and C. H. Chen, "Balanced coupled-resonator bandpass filters using multisection resonators for common-mode suppression and stopband extension," *IEEE Trans. Microwave Theory Tech.*, Vol. 55, No. 8, 2007.
11. Gupta, K. C., R. Garg, I. Bahl, and P. Bhartia, "Microstrip discontinuities I," *Microstrip lines and Slot lines*, 2nd Edition, 196–200, Artech House, London, 1996.
12. Hong, J. S. and M. J. Lancaster, "Cross-coupled microstrip hairpin resonator filters," *IEEE Trans. Microwave Theory Tech.*, Vol. 46, 118–122, 1998.
13. Hong, J. S. and M. J. Lancaster, "Coupled resonator circuits," *Microstrip Filters for RF/Microwave Applications*, 247–249, Wiley Inter Science, NY, 2016.
14. Weber, R. J. and Q. Song, "Introduction to microwave circuits. radio frequency and design applications," *IEEE Press Series on RF and Microwave Technology*, ISBN 0-7803-4704-8, 2001.
15. White Paper, "Balanced device characterization," *Agilent Technologies*, [Online] Available at www.keysight.com/upload/cmc_upload/All/EPSG084733.pdf.